ContamLD: Estimation of Ancient Nuclear DNA Contamination Using Breakdown of Linkage Disequilibrium

Nathan Nakatsuka[1,2,3,*,†], Éadaoin Harney[1,3,4,*,†], Swapan Mallick[1,3], Matthew Mah[1,3], Nick Patterson[3], David Reich[1,3,5,6,†]

[1]Department of Genetics, Harvard Medical School, New Research Building, 77 Ave. Louis Pasteur, Boston, MA 02115, USA
[2]Harvard-MIT Division of Health Sciences and Technology, Harvard Medical School, Boston, MA 02115, USA
[3]Department of Human Evolutionary Biology, Harvard University, 16 Divinity Ave., Cambridge, MA 02138, USA
[4]Department of Organismic and Evolutionary Biology, Harvard University, 16 Divinity Ave., Cambridge, MA 02138, USA
[5]Broad Institute of Harvard and Massachusetts Institute of Technology, Cambridge, MA 02141, USA
[6]Howard Hughes Medical Institute, Harvard Medical School, Boston, MA 02115, USA

*co-first authors

[†] Corresponding authors: Nathan Nakatsuka (nathan_nakatsuka@hms.harvard.edu), Éadaoin Harney (harney@g.harvard.edu), and David Reich (reich@genetics.med.harvard.edu)

Abstract

Ancient DNA (aDNA) has emerged as a powerful technology for learning about history and biology, but unfortunately it is highly susceptible to contamination. Here we report a method called *ContamLD* for estimating autosomal aDNA contamination by measuring the breakdown of linkage disequilibrium in a sequenced individual due to the introduction of contaminant DNA, leveraging the idea that the contaminant should have haplotypes that are uncorrelated to those of the studied individual. Using simulated data, we confirm that *ContamLD* accurately infers contamination rates with low standard errors (e.g. less than 1.5% standard error in cases with <10% contamination and data from at least 500,000 sequences covering SNPs). This method is optimized for application to aDNA, leveraging characteristic aDNA damage patterns to provide calibrated contamination estimates. Availability: https://github.com/nathan-nakatsuka/ContamLD.

Keywords

Ancient DNA, linkage disequilbrium, contamination

Background

Ancient DNA (aDNA) has emerged as a powerful technology for inferring population history, allowing direct study of the genomes of individuals who lived thousands of years in the past (1-3). Unfortunately, these inferences can be distorted by contamination during the excavation and storage of skeletal material, as well as the intensive processing required to extract the DNA and convert it into a form that can be sequenced.

62

63 Accurate measurement of the proportion of contamination in ancient DNA data is important,
64 because it can provide guidance about whether analysis should be restricted to sequences that
65 show the characteristic C-to-T damage pattern of authentic aDNA (if contamination is high) (4),
66 or carried out at all. When analysis is restricted to focus only on damaged sequences, large
67 fractions of authentic sequences are usually removed from the analysis dataset, as only a
68 fraction of genuinely ancient sequences typically carry characteristic damage. In addition, if a
69 sample is contaminated by another individual with damaged DNA—which can arise for example
70 as a result of cross-contamination from other specimens handled in the same ancient DNA
71 laboratory—it is impossible to distinguish authentic sequences from contaminating ones based
72 on the presence or absence of characteristic ancient DNA damage.

73

74 Current methods for estimating contamination have significant limitations. Methods based on
75 testing for heterogeneity in mitochondrial DNA sequences (which are expected to be
76 homogeneous in an uncontaminated individual) can be biased, because there are several
77 orders of magnitude of variation in the ratio of the mitochondrial to nuclear DNA copy number
78 across samples. Thus, samples that have evidence of mitochondrial contamination can be
79 nearly uncontaminated in their nuclear DNA, while samples that have no evidence of
80 mitochondrial contamination can have high nuclear contamination (5). Another reliable method
81 for estimating rates of contamination in ancient DNA leverages polymorphism on the X
82 chromosome in males (*ANGSD*), but this method does not work in females (6-8).

83

84 Several methods for estimating contamination rates in present-day nuclear DNA have been
85 published, including *ContEst* (9) and *ContaminationDetection* (10). However, these methods
86 generally assume access to uncontaminated genotype data from the individual of interest or
87 access to all possible contaminating individuals, which is rarely available for aDNA. Another

88 method developed specifically for aDNA, *DICE*, jointly estimates contamination rate and error
89 rate along with demographic history based on allele frequency correlation patterns (11).
90 However, this method requires both explicit demographic modeling and high genome coverage.
91 While this may be effective for estimation of contamination in archaic genomes like
92 Neanderthals and Denisovans that are highly genetically diverged from likely contaminant
93 individuals, it is not optimized for study of contamination among closely related present-day
94 human groups with complex demographic relationships or individuals from the same population.
95 In Racimo *et al.* 2016 (11), *DICE* required over 3x genome sequence coverage and solved the
96 distinctive problem of measuring contamination of present-day human in a Neanderthal
97 genome.
98
99 We report a method for estimating autosomal aDNA contamination using patterns of linkage
100 disequilibrium (LD) within a sample. This approach, called *ContamLD*, is based on the idea that
101 when sequences from one or more contaminating individuals are present in a sample, LD
102 among sequences derived from that sample is expected to be diminished, because the
103 contaminant DNA derives from different haplotypes and therefore should have no LD with the
104 authentic DNA of the ancient individual of interest. Thus, the goal of the algorithm is to
105 determine the LD pattern the ancient individual would have had without contamination and
106 compare it to the LD pattern found in the sample. The LD patterns of ancient individuals are
107 determined using reference panels from 1000 Genomes Project populations to compute
108 approximate background haplotype frequencies where haplotypes are defined as pairs of SNPs
109 with high correlation to each other. Contamination is then estimated by fitting a maximum
110 likelihood model of a mixture of haplotypes from an uncontaminated individual and a proportion
111 of contamination (to be estimated from the data) from an unrelated individual. *ContamLD*
112 corrects for mismatch of the ancestry of the ancient individual with the reference panels using
113 two different user-specified options. In the first option, mismatch is corrected using estimates

from damaged sequences (which, in principle, lack present-day contaminants). In the second option, *ContamLD* performs an “external” correction by subtracting the sample’s contamination estimate from estimates for individuals of the same population believed to have negligible contamination (the user could obtain this value from a *ContamLD* calculation on a male individual with a very low estimate of contamination based on *ANGSD*). The second option has more power than the first option and allows detection of cross-contamination by other ancient samples, but it could have biases if a good estimate of an un-contaminated individual from the same population is not available for the external correction.

We show that *ContamLD* accurately infers contamination in both ancient and present-day individuals of widely divergent ancestries with simulated contamination coming from individuals of different ancestries. The contamination estimates are highly correlated with estimates based on X chromosome analysis in ancient samples that are male, as assessed using the tool *ANGSD* (12). *ContamLD* run with the first option has standard errors less than 1.5% in samples with at least 500,000 sequences covering SNPs (~0.5x coverage for data produced by in-solution enrichment for ~1.2 million SNPs (2, 13), or ~0.1x coverage for data produced using whole-genome shotgun sequences), while the second option has standard errors less than 0.5% in these situations, allowing users to detect samples with 5% or more contamination with high confidence so they can be removed from subsequent analyses.

Results

Simulations of Contamination in Present-Day Individuals:

To test the performance of *ContamLD*, we simulated sequence level genetic data. For our first simulations, each uncontaminated individual was based on genotype calls from a present-day

140 individual from the 1000 Genomes Project dataset. To determine the sequence coverage at
141 each site, we used genome data from a representative ancient individual of 1.02x coverage and
142 in each case generated the same number of simulated sequences at each site, with allele type
143 corresponding to that of the present-day individual (i.e. if the present day individual is
144 homozygous reference at a site, all simulated alleles are of the reference type, while if the
145 present day individual is heterozygous, simulated alleles are either of the reference or
146 alternative type, with 50% probability of each). The damage status (i.e. whether it carries the
147 characteristic C-to-T damage often observed in ancient DNA sequences) of each sequence was
148 also determined based on the status of the ancient reference individual. Contaminating
149 sequences were then "spiked-in" at varying proportions (0 to 40%), using an additional present-
150 day individual from the 1000 Genomes Project to determine the contaminating allele type (see
151 Methods). All contaminating sequences were defined to be undamaged, consistent with
152 contamination coming from a non-ancient source.
153
154 For most of the analyses reported in this study, we simulate data for SNP sites defined on the
155 1.24 million SNP capture reagent (2, 13) that intersect with 1000 Genomes sites, after removing
156 sex chromosome sites (leaving ~1.1 million SNPs). However, our software allows users to make
157 panels based on their own SNP sets, and in a later section we report results from a larger panel
158 (~5.6 million SNPs) provided with the software that can be used with shotgun sequenced
159 samples, which has more power to measure contamination.
160
161 We first analyzed data generated using a reference individual from the 1000 Genomes CEU
162 population (Utah Residents (CEPH) with Northern and Western European Ancestry) and the
163 SNP coverage profile of a 1.02x coverage ancient West Eurasian individual (I3756; see
164 Methods). Supplementary Figure 1 illustrates the distribution of LOD (logarithm of the odds)
165 scores generated when the algorithm is run on samples with 0%, 7% and 15% simulated

contamination. Supplementary Figure 2 shows all the estimates from 0 to 40%. At very high contamination (above 15%) *ContamLD* often overestimates the contamination rate, but in practice samples with above 10% contamination are generally removed from population genetic analyses, so inaccuracies in the estimates at these levels are not a concern in our view (the importance of a contamination estimate in many cases is to flag problematic samples, not to be able to accurately estimate the contamination proportion). *ContamLD* assumes that the individual making up the majority of the sequences is the base individual, so we do not explore contamination rates greater than 50% in these simulation studies.

We observe a linear shift in the contamination estimates such that most estimates are biased to be slightly higher than the actual value, with even greater overestimates occurring at higher contamination rates (Supplementary Figure 2). This is likely due to the difference between the haplotype distribution of the test individual and that of the haplotype panel, as the magnitude of this shift increases as the test individual increases in genetic distance from the haplotype panel. Even in cases where the test individual is of the same ancestry as the haplotype panel (as in Supplementary Figure 2) there is expected to be a shift, because the test individual's haplotypes are a particular sampling of the population's haplotypes, and the difference between having only frequencies of the haplotype panel and a particular instantiation of those frequencies in the test individual will lead to the artificial need for an external source ("contaminant") to fit the model properly. Further, we observe negative shifts for inbred individuals, as expected because the algorithm assumes the paternal and maternal copy of a chromosome are unrelated; if they are related, then extra LD will be induced and more contamination will be necessary to lead to the expected LD pattern. In principle, this inbreeding effect be corrected explicitly by estimating the total amount of ROH in each individual and applying this as a correction, although we do not provide such functionality as part of our software as there is not yet a reliable methodology for

quantifying the proportion of the genome that is affected by inbreeding in ancient individuals. In any case, a correction will always be necessary to address these biases.

In our implementation, we correct for these shifts in two ways, implemented as different options in *ContamLD*. The first option leverages sequences that contain C-to-T damage that is characteristic of ancient sequences. This option assumes these sequences are authentically ancient and not derived from a contaminating source (assumed to be from present-day individuals), so the *ContamLD* estimate based on un-damaged sequences is corrected by estimates based on the damaged sequences (see Methods for more details). In the second option, we allow the user to subtract the contamination estimate from the estimate of an individual of the same ancestry assumed to be uncontaminated. The second option has smaller standard errors than the first option (Figure 1), because it does not rely on estimates from damaged sequences (which have less power since they are a much smaller subset of the data). In addition, the second option allows one to estimate contamination in cases where the source of contamination is also ancient in origin (i.e. a contamination event that occurred anciently or due to cross contamination with other ancient samples), while the first option will likely produce an underestimate in these cases, since it assumes that sequences that contain C-to-T damage are not contaminated. However, the second option will generally not be reliable unless there is a relatively high coverage, ancestry-matched external sample for correction (with no inbreeding in either the sample of interest or the external sample). The rest of the analyses were based on the first option, but *ContamLD* includes both methods as options, and the uncorrected score forms the basis for warnings outputted by the software (e.g. high contamination or possible contamination with another ancient sample leading to an inaccurate damage correction estimate).

217 **A)** **B)**

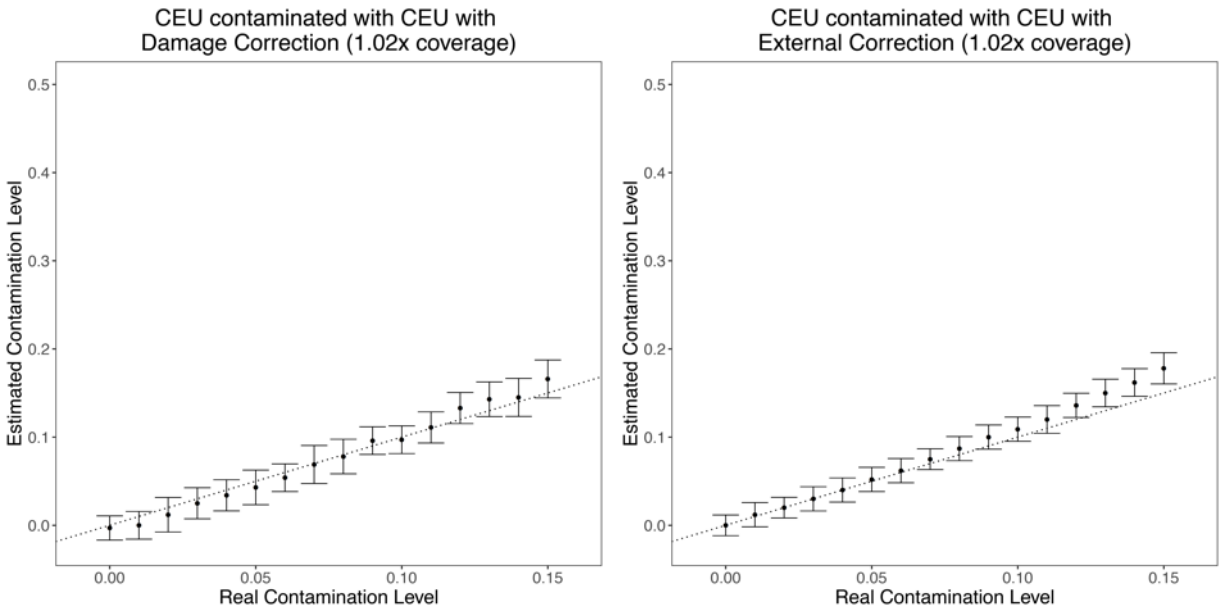

218

219 **Figure 1. *ContamLD* estimates when the uncontaminated source, contaminant source, and**
220 **haplotype panel are all from the same population (CEU).** Contamination estimates when the simulated
221 contamination rate is between 0.00-0.15. **A)** Estimates with damage restricted correction (option 1). **B)**
222 Estimates with external correction from an uncontaminated sample (option 2). The black dotted line is
223 y=x, which would correspond to a perfect estimation of contamination. Error bars are 1.96*standard error
224 (95% confidence interval).

225

226 *Simulated Contamination of Ancient Samples with Present-Day Samples:*

227 *ContamLD* is designed to work on ancient individuals, so we simulated contamination of real
228 ancient individuals with present-day individuals from the 1000 Genomes Project, a scenario that
229 would occur when skeletal material from ancient individuals is contaminated by present-day
230 individuals during excavation or some point of the processing of the material. We used male
231 individuals with very low contamination rates (less than 1% based on X chromosome estimates
232 using *ANGSD* (12), which we subtracted from the *ContamLD* estimates to correct for any
233 underlying contamination). Figure 2A shows results from an Iberian Bronze Age sample (14)
234 (I3756) that has approximately 1.02x coverage at the targeted ~1.24 million SNP positions,

demonstrating that *ContamLD* produces highly accurate contamination estimates for this simulation.

Effect of Different Haplotype Panels

There are many potential cases in which ancient individuals can come from populations with very different genetic profiles to present-day 1000 Genomes populations, leading to an ancestry mis-match to the haplotype reference panels. *ContamLD* provides panels from all 1000 Genomes populations as well as tools to identify the panel most closely matching to the ancestry of their ancient individual, which they can then select for the analysis. However, due to the potential for ancestry mis-match to still occur, we tested the effect of choosing haplotype panels that are genetically diverged from the individual of interest (Figure 2A). For the ancient Iberian sample, the CEU and TSI (Toscani in Italia) panels—representing northern and southern European ancestry, respectively—yielded contamination estimates that are close to the true contamination rate, especially for rates below 5%. However, *ContamLD* underestimates contamination by ~2% when the CHB (Han Chinese in Beijing, China) and YRI (Yoruba in Ibadan, Nigeria) panels were used instead (though we view these as unlikely cases, because the user should usually be able to choose a panel more closely related to their ancient individual than these scenarios). We thus recommend that users take care to choose an appropriate panel that is within the same continental ancestry as their ancient individual. Nevertheless, we note that we were able to obtain reasonably accurate estimates for Upper Paleolithic European hunter-gatherers, such as the Kostenki14 individual (15), who is ~37,470 years old, even when using present-day European panels that have significantly different ancestry from the hunter-gatherers (Supplementary Figure 3).

A)

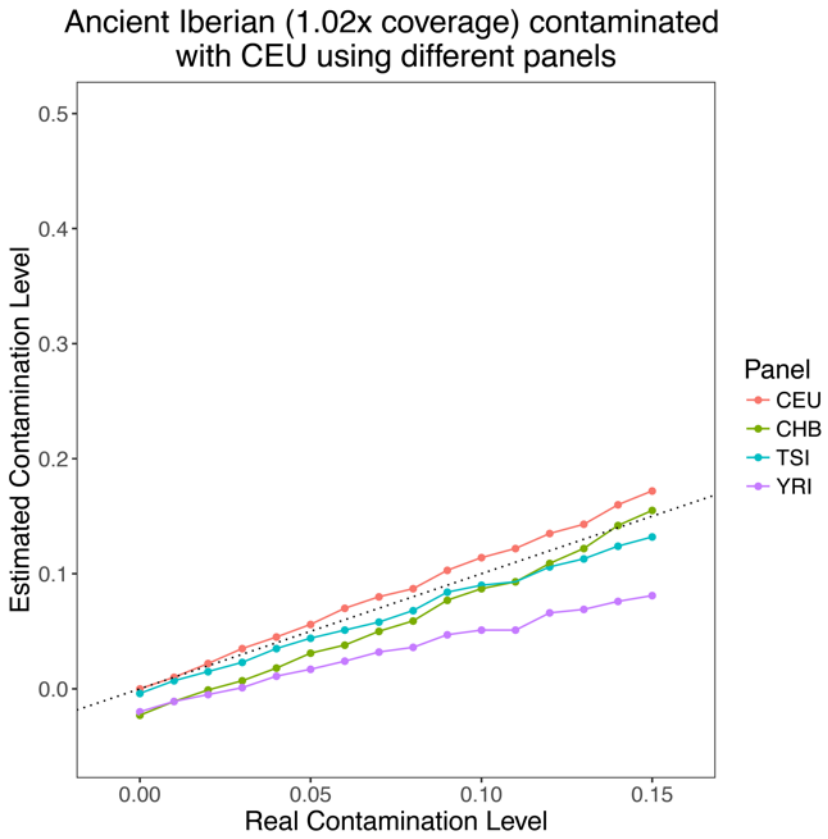
Ancient Iberian (1.02x coverage) contaminated with CEU using different panels
Estimated Contamination Level
Real Contamination Level
0.0
0.1
0.2
0.3
0.4
0.5
0.00
0.05
0.10
0.15
Panel
CEU
CHB
TSI
YRI

B)

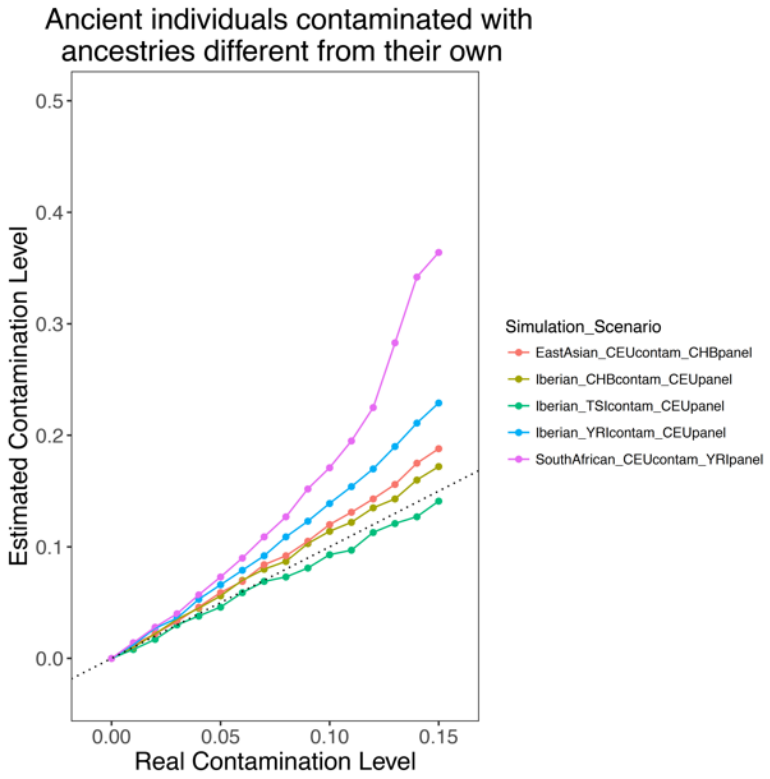
Ancient individuals contaminated with ancestries different from their own
Estimated Contamination Level
Real Contamination Level
0.0
0.1
0.2
0.3
0.4
0.5
0.00
0.05
0.10
0.15
Simulation_Scenario
EastAsian_CEUcontam_CHBpanel
Iberian_CHBcontam_CEUpanel
Iberian_TSIcontam_CEUpanel
Iberian_YRIcontam_CEUpanel
SouthAfrican_CEUcontam_YRIpanel

264 **Figure 2. Genetic distance between uncontaminated individual and contamination sources or**
265 **haplotype panels impacts *ContamLD* estimates A)** Ancient Iberian (I3756, 1.02x coverage)
266 contaminated with CEU with haplotype panels generated from CEU, TSI, CHB, and YRI populations. **B)**
267 Contamination estimates from the same ancient Iberian contaminated with TSI, CHB, or YRI and
268 analyzed with a CEU panel, from an ancient East Asian (DA362.SG, 1.10x coverage) contaminated with
269 CEU and analyzed with a CHB panel, or from an ancient South African (I9028.SG, 1.21x coverage)
270 contaminated with CEU and analyzed with a YRI panel. The black dotted line is y=x, which would
271 correspond to a perfect estimation of the contamination. All samples had damage restricted correction
272 applied (option 1).
273
274 *Effect of Mismatch Between the Ancestry of the True Sample and Contaminating Individual*
275 Contamination can come from a wide variety of sources, including, but not limited to, different
276 members of the archaeological excavation team, the aDNA laboratory, or even residual human
277 DNA on the plastic and glassware. Thus, we sought to understand the effect of mismatch in the
278 ancestry of the true sample and the contaminating individual in our contamination estimates. We
279 found that as the ancestry of the two diverged, *ContamLD* over-estimated contamination (Figure
280 2B). This effect occurred when we tested an ancient European with different contaminant
281 ancestries as well as when we tested ancient East Asian (16) and ancient South African (17)
282 samples contaminated with European DNA. Nevertheless, the over-estimation was not severe
283 at contamination levels below 5 percent, and samples above this proportion would likely be
284 flagged as problematic. We also explored scenarios where the ancestry of the panel matches
285 the contaminant rather than the true sample (Supplementary Figure 4) and found a ~2% under-
286 estimate at low levels of contamination and an over-estimate at high levels of contamination,
287 which we view as not problematic in practice for the same reasons as in the scenarios above.
288 When we tested the effect of having multiple contaminant individuals (Supplementary Figure 5),
289 we found no significant difference relative to having a single contaminant individual.

290

291 *Effect of Coverage:*

292 We tested the power of our procedure at different coverages (Figure 3). We found that while our
293 estimates were not biased to produce estimates consistently above or below the true value, the
294 standard errors increased significantly at lower coverages, as expected for the decreased power
295 for accurate estimation in these scenarios. We provide a much larger panel with ~5.6 million
296 SNPs (vs. ~1.1 million for the 1240K panel) that improves accuracy and usually decreases
297 standard errors for samples that are shotgun sequenced (Supplementary Figure 6). This panel
298 increases *ContamLD*'s compute time and memory requirements, though, so we recommend
299 that it only be used for individuals with lower than 0.5x coverage. In addition, we provide users
300 tools to create their own panels to meet their specific needs.

301

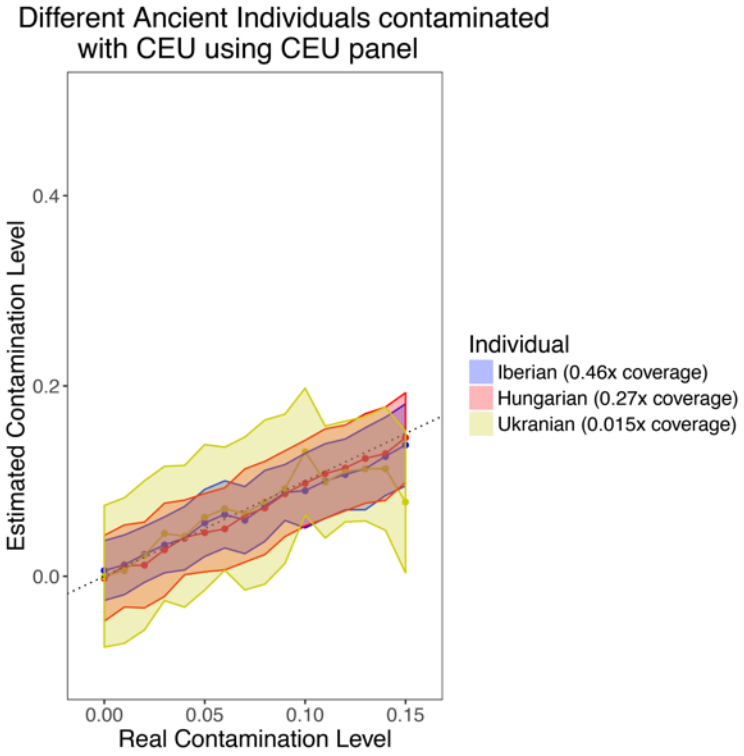

302

303 **Figure 3. *ContamLD* estimates for ancient European samples of different coverages after damage**
304 **restricted correction (option 1).** An ancient Iberian of 0.46x coverage, an ancient Hungarian of 0.27x

305 coverage, and an ancient Ukranian of 0.015x coverage (~16,000 snps) were contaminated with CEU and
306 analyzed using a CEU panel with *ContamLD* option 1 (damage restricted correction). The black dotted
307 line is y=x. Error shading is 1.96*standard error (95% confidence interval).
308
309 *Estimating Contamination in Admixed Individuals*
310 *ContamLD* relies on measuring the difference between the LD pattern of the sample and that
311 expected from an uncontaminated individual. However, individuals from groups recently
312 admixed between two highly divergent ancestral groups have LD patterns, in principle, similar to
313 that of an unadmixed individual with contamination from a group with ancestry diverged from
314 that of the individual of interest. To determine how this would impact *ContamLD*, we ran the
315 software on an ASW (Americans of African Ancestry in Southwest USA) individual with different
316 levels of added CEU contamination. When we ran *ContamLD* with a YRI panel and no
317 correction on an individual with no contamination, the individual was inferred to have a
318 contamination of ~20% (likely because the individual had ~15% European ancestry, and this
319 was interpreted by the software as contamination). Using an ASW panel did not perform any
320 better. However, the concerns were mostly addressed by the damage-restricted correction
321 (option 1) at low contamination levels (Supplementary Figure 7). The simulation with African-
322 Americans represents an extreme of difficulty, because the individual is from a group with very
323 recent admixture (~6 generations (18)) of ancestries highly divergent from each other with one
324 of the ancestries very genetically similar to the reference panel. It highlights how the damage-
325 restricted correction is still able to produce accurate estimates in these difficult cases.
326
327 *Simulations to Compare ContamLD to ANGSD X Chromosome Estimates*
328 We performed simulations where we randomly added sequences at increasing levels from 0 to
329 15% from an ancient West Eurasian individual (I10895) into the BAM files of 65 ancient male
330 individuals of variable ancestries and ages (we set the damaged sequences to be only from the

331 non-contaminant individual; see Methods). We chose ancient male individuals that had average
332 coverage over 0.5X and X chromosome contamination estimates under 2% (using method 1 of
333 *ANGSD*) when no artificial contamination was added (and also corrected even for this baseline
334 contamination by setting damaged reads to be a 5% down-sampling of the files that had no
335 artificial contamination; see Methods). We then analyzed the individuals with *ContamLD* and
336 *ANGSD* and found that compared to *ANGSD*, *ContamLD* consistently had the same or lower
337 errors relative to the real contamination level (Figure 4, Supplementary Online Table 2).
338

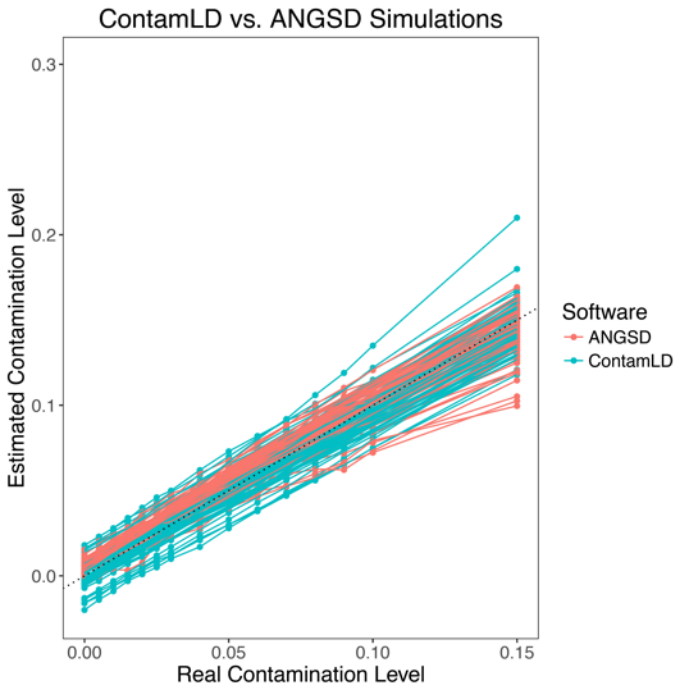

339

340 **Figure 4. Contamination estimates with *ContamLD* and *ANGSD* for ancient individuals with**
341 **different levels of contamination added in.** 65 ancient individuals with average coverage over 0.5X had
342 increasing levels of artificial contamination added in (from I10895, an ~1200BP ancient West Eurasian
343 individual) and were then analyzed with *ContamLD* (with panels most genetically similar to the ancient
344 individual and using damage restricted correction, option 1) and *ANGSD*. Details of all estimates
345 (including standard errors) are provided in Supplementary Online Table 2. The black dotted line is y=x,
346 which would correspond to a perfect estimation of the contamination.
347

348 *Comparing ContamLD, ANGSD, and Mitochondrial Estimates (ContamMix) in Ancient*
349 *Individuals without Added Contamination*
350 We tested 439 ancient males with *ContamLD*, *ANGSD* (X chromosome contamination
351 estimates), and *ContamMix* (mitochondrial contamination estimates) without adding additional
352 contamination. For this analysis, we included published data generated with the ~1.24 million
353 SNP enrichment reagent, as well as data from the same sites that failed quality control due to
354 evidence of contamination (Supplementary Online Table 3). Similar to prior studies (5), the
355 mitochondrial estimates often differed from the nuclear (*ANGSD* and *ContamLD*) estimates,
356 showing high contamination in some samples that had low nuclear contamination, and low
357 mitochondrial contamination in some samples that had high nuclear contamination (Figure 5a).
358 In contrast, *ANGSD* and *ContamLD* had better concordance. However, we observed that some
359 of the samples with high contamination estimates based on *ANGSD* had much lower *ContamLD*
360 estimates, reflecting over-correction from analyzing the damaged sequences, perhaps because
361 the contamination was actually cross-contamination from other ancient individuals, violating the
362 assumptions of our damage-correction (Figure 5b). This problem was mitigated in part,
363 however, because *ContamLD* produces a warning of "Very_High_Contamination" if the
364 uncorrected estimate is above 15% (even in cases where the corrected estimate is very low),
365 and all samples with X chromosome estimates over 5% were flagged with this warning and/or
366 had estimates of over 5% contamination with *ContamLD* (all samples with less than 5%
367 contamination in *ANGSD* had lower than 5% contamination with *ContamLD*). It is unfortunately
368 not possible to know the true contamination of the samples we tested in Figure 5, but the fact
369 that our software produced results with good correlation to X chromosome estimates shows that
370 it works well in real ancient data.
371 It is possible for there to be samples with moderately high contamination from another
372 ancient individual but both a low damage restricted correction estimate and no warning
373 generated, because these would have high uncorrected estimates, yet not high enough to reach

the threshold required for the warning. These samples would have to be identified with an external correction. Lowering the threshold for the “Very_High_Contamination” warning would produce too many false positives, because there are many cases with high uncorrected estimates that have low corrected estimates that are likely not contaminated (e.g. due to ancestry mismatches of the panel and the test individual). To understand these issues better, we performed a simulation in which an ancient Iberian (I3756) was contaminated with another ancient West Eurasian individual (I10895) and the damaged sequences were set to be a 5% down-sampling of the set of contaminated sequences (thus simulating a case in which all of the contamination is from another ancient individual who has the same damage proportion as the ancient individual of interest). We found that, as expected, the contamination from the ancient individual was not detected (the contamination estimates were always near 0%) by the damage restricted correction version of *ContamLD* until the contamination reached 15% at which point the “Very_High_Contamination” flag came up (Supplementary Figure 8). The contamination would have been detected with the external correction version of *ContamLD* (since the damage restricted correction continued to go up with increasing contamination; see Supplementary Online Table 4), but without an uncontaminated ancient individual of the same group as the target individual, this would be difficult to do without the possibility of bias in the contamination estimate.

400 **(A)** **(B)**

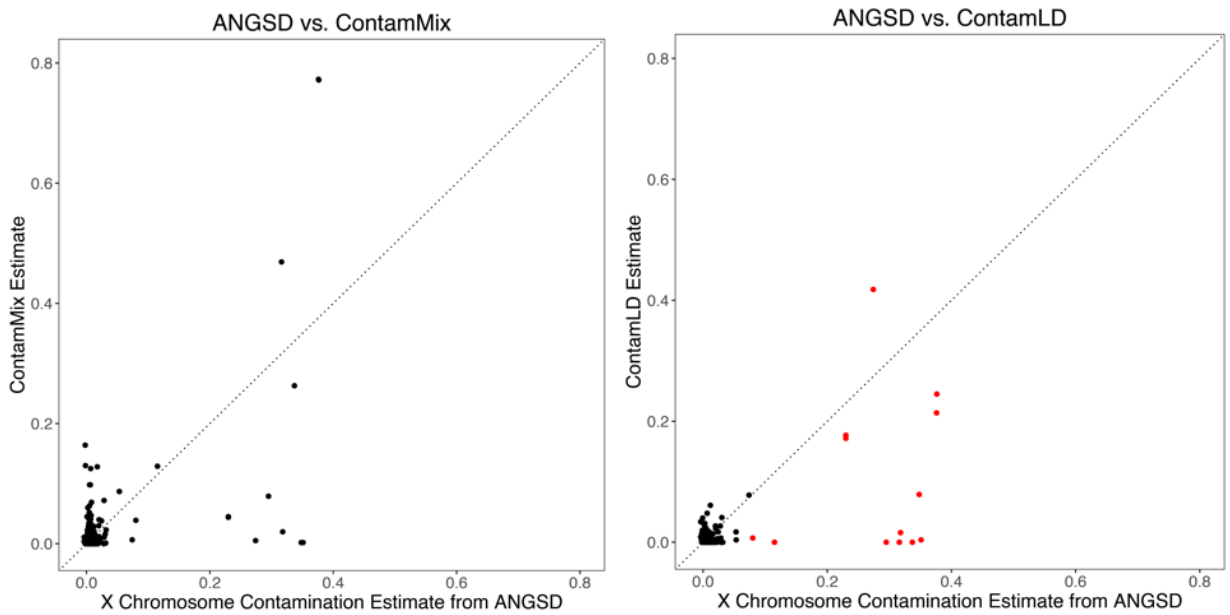

401

402 **Figure 5. Contamination estimates from *ContamLD*, *ANGSD*, and *ContamMix* in 439 ancient**
403 **individuals of variable ancestry.** *ANGSD* estimates are plotted on the X-axis, and on the Y-axis are
404 either **(A)** *ContamMix* or **(B)** *ContamLD* estimates. In red are samples that were flagged in *ContamLD* as
405 "Very_High_Contamination" based on having uncorrected estimates over 15%. All *ContamLD* estimates
406 below 0 were set to 0.

407

408 # Discussion and Conclusion

409 We have presented a tool, *ContamLD*, for estimating rates of autosomal DNA contamination in
410 aDNA samples. *ContamLD* is able to measure contamination accurately in samples of both
411 male and female individuals, with standard errors less than 1.5% for individuals with coverage
412 above 0.5X on the 1240K SNP set (for contamination levels less than 10%) for the damage
413 restricted correction version (option 1). On the shotgun panel we provide, standard errors are
414 less than 1.5% for coverages above 0.1x. *ContamLD* is best suited to scenarios in which the
415 contaminant and the ancient individual of interest are similar ancestry, which is useful, because
416 *DICE* (11) and many population genetic tools (e.g. PCA or ADMIXTURE (19)) are better suited

417 for detecting cases where the contaminant is of very different ancestry from the ancient
418 individual of interest. *ContamLD* works even for recently admixed individuals. Lastly, *ContamLD*
419 can detect cases of contamination from other ancient individuals, though this works best if it is
420 large amounts of contamination that can reach the threshold required for the
421 "Very_High_Contamination" flag.
422
423 We tested *ContamLD* in multiple different simulation scenarios to determine when bias or less
424 reliable results would occur. When applied to the situation with a test individual (ancient or
425 present-day), contaminant, and haplotype reference panel all from the same continental
426 ancestry, *ContamLD* provides an accurate, un-biased estimate of the contamination. When the
427 contaminant comes from a population that is of a different continental ancestry from the
428 population used for the base and haplotype panel, the contamination appears to be slightly
429 overestimated, particularly for higher contaminations. This should not be a large problem in
430 analyses of real (i.e. non-simulated) data, however, because the effect is small at the
431 contamination levels of interest (<5%). When we varied haplotype panels, we found that the
432 estimator is robust when applied to simulated datasets using haplotype panels that are
433 moderately divergent from the base sample (within-continent variation). We provide users tools
434 for automatically determining the panel that shared the most genetic drift with the sample so that
435 the user can use the panel most closely related to the sample. In other simulations, we found
436 that the performance of the algorithm declines as the coverage of the sample decreases. The
437 estimates are not unbiased, but the standard errors significantly increase when fewer than
438 300,000 sequences are available for analysis. In these cases, if the individual was shotgun
439 sequenced, we recommend that users choose the shotgun panel, which will substantially
440 increase power for the analyses.
441

442 We applied the algorithm to estimate contamination levels in dozens of ancient samples and
443 compared them to X chromosome based contamination estimates. There was generally good
444 correlation with the X chromosome estimates, except that when contamination was very high,
445 the LD based estimates were sometimes estimated incorrectly due to over-correction from the
446 damage estimates. This problem is mitigated, however, because the software indicates if the
447 uncorrected estimate is very high so users can identify highly contaminated samples and
448 remove them from further analyses. A difficult case for the software is if there is contamination
449 in part from another ancient sample. This can cause an over-correction and lead to an under-
450 estimate of the contamination. The "Very_High_Contamination" warning catches very high
451 contamination from other ancient samples, but it will miss cases of moderate levels of
452 contamination from other ancient samples, because it will not reach the threshold required for
453 the warning. In theory, the user can determine the true contamination in these cases using the
454 external correction, but the external correction can be difficult if the user does not have an
455 adequate sample to correct the estimate of the sample of interest. The damage correction of the
456 software also does not work if the samples have undergone full UDG treatment (no damaged
457 sequences), and for this case, the external correction is the only option.
458
459 The software run-time is dependent on the SNP coverage. If ~1,000,000 SNPs are covered (the
460 depth of the coverage on each SNP does not affect run-time), the full analysis for the sample
461 will be approximately 2 hours if 3 cores are available on CentOS 7.2.15 Linux machines (~25
462 GB of memory). The software is designed for samples to be run in parallel, so the total time for
463 analysis even for large numbers of samples is often not much greater than the time for a single
464 sample.
465
466 In summary, *ContamLD* is able to estimate autosomal nuclear contamination in ancient DNA
467 accurately with standard errors that depend on the coverage of the sample. This will be

468 particularly useful for female samples where X chromosome estimates are not possible. As a
469 general recommendation for users, we believe in most cases all samples with a contamination
470 estimate that is greater than 0.05 (5%) should be removed from further analyses, or the
471 contamination should be explicitly modeled in population genetic tests.

472

Supplementary Data:

Supplementary Data include an Excel spreadsheet detailing all ancient samples used and the contamination estimates for this algorithm. Also included are 8 supplementary figures.

Materials and Methods

Datasets:

Present-day samples:

Genome wide data from the 1000 Genomes Project dataset (20) were used as present-day reference samples. We restricted to sites included in the aDNA ~1.24 million SNP capture reagent (2, 13) and to SNPs at greater than 10% minor allele frequency in the 1000 Genomes Project dataset (20). However, the software allows users to make panels based on their own SNP set. In the analyses presented here, we filtered for SNPs that were present in the 1000 Genomes dataset and also removed all sex chromosome SNPs leading to 1,085,678 SNPs in the final 1240K dataset and 5,633,773 SNPs in the final shotgun dataset.

Ancient samples:

We analyzed mitochondrial and X chromosome contamination estimates (12, 21) from ancient individuals from previous studies generated by shotgun sequencing or targeted enrichment with 1.24 million SNP enrichment, including many samples that failed quality control due to contamination but were from the same archaeological sites (2, 17, 22-28). Information about the ancient individual data are detailed in Supplementary Online Table 1 and below.

498 *Obtaining sequence information:*

499 For each ancient individual, we generated the sequence-depth data from the sample bam file,
500 counting the number of reference and alternative alleles at each SNP site in the analysis
501 dataset. Damage-restricted data was generated by restricting to sequences with PMD scores
502 greater than or equal to 3 (4). Our software can accommodate both genotype call data as well
503 as sequence data (the sequence data adds additional power to the analyses), but all analyses
504 were performed using the sequence-based method. We provide users with tools to pull down
505 read count data from BAM files in the format required for *ContamLD*.

506

507 **Haplotype Calculation**

508

509 To create haplotype panels, we obtained all SNP pairs in high LD for each 1000 Genomes
510 population using PLINK version 1.9 (29) with r^2 cut-off of 0.2. (Users can increase power slightly
511 at the expense of increased computational time by creating their own haplotype panel with a
512 lower r^2 cutoff). We then calculated the frequencies of each SNP in all of these pairs as well as
513 the haplotype frequencies at each of these pairs while holding out the present-day individuals
514 used for contamination simulation.

515

516 **Algorithm to Estimate Contamination**

517

518 Our goal is to estimate α, the level of contamination, by examining the frequencies of SNP pairs
519 that should be in LD (we term this two-SNP pair a haplotype) and determining how much their
520 frequencies differ from what would be expected under no contamination. To estimate this, we
521 need both the distribution underlying the haplotypes (q) that an uncontaminated test sample
522 should have as well as the distribution of ”unrelated haplotypes” (p) that would form by chance
523 from background allele frequencies.

524

To determine *q* we must account for the fact that the test individual's genotypes are not phased. Due to the low sequence depths at each SNP in ancient DNA, it is difficult to make confident heterozygous calls, so instead we create pseudo-haploid calls by randomly choosing a sequence to represent the genotype at that position (this holds when we are using genotype calls or the sequence information directly, and when multiple sequences cover the same SNP, we use all of them and treat them as independent). Thus, for this analysis, when examining a pair of SNPs, it is equally likely for the SNP pair to have been formed from the true haplotype (if the same parental chromosome is sampled from in both SNPs of the haplotype) or the background distribution (if the opposite parental chromosome is sampled from). We therefore can estimate *q* as:

$$q = p/2 + \widetilde{p}/2$$

where $\tilde{p}$ is the distribution of true haplotypes and *p* is the distribution of unrelated haplotypes that would form by chance from background allele frequencies. For inbred samples, the weight on $\tilde{p}$ is more than 1/2, because the two parental chromosomes are more related, but this can generally be corrected (see below).

$\tilde{p}$ can be estimated from an external reference panel using a maximum likelihood estimator (MLE). This would be:

$$log(L(h|c)) = \sum_{j=1}^{n} \sum_{i=1}^{4} c_{ij} log(P(i,j|h))$$

with:

$$P(i,j|h) = \sum_{a_1,a_2,b_1,b_2=0,1;a,b\rightarrow(i,j)} h_{(a_1,b_1)} * h_{(a_2,b_2)}$$

where $P(i, j|h)$ is the (unknown) diploid count distribution of the haplotypes of the test individual, n is the number of SNP pairs, c is the vector of observed haplotypes in the diploid count panel, i sums over all 4 haplotype possibilities, $h_{(a,b)}$ are the (also unknown) haplotype distributions of the parents of the test individual, and $a, b \rightarrow (i, j)$ implies that $a_1 + a_2 = i$ and $b_1 + b_2 = j$, meaning that one adds up all cases where the haplotype combination would lead to a particular diploid count (e.g. in the notation, for example, 01,11 means the first parent contributes a haplotype that has 0 alternative alleles at the first SNP and 1 alternative allele at the second SNP, and the second parent contributes a haplotype where both SNPs have the alternative allele. The test individual with these parents would then have a 12 diploid count, which means at the first SNP the individual has 1 alternative allele and at the second SNP the individual has 2 alternative alleles. Since our observed data are not phased, both 01,11 and 11,01 would lead to a 12 diploid count). This assumes independence of SNP pairs, which is not true, but because our standard errors are based on jackknife resampling across chromosomes, this assumption does not bias the error estimates.

The MLE would be computationally intractable to solve due to our lack of knowledge of which parent contributed to each count, so we instead used a simple EM algorithm to obtain h. The algorithm involved an expectation step of:

$$n_1 = \frac{C_{(i,j)} * \sum_{a,b \rightarrow (i,j)} h_{(a,b)} * h_{(a_2,b_2)}}{P(i,j|h)}$$

where n_1 is the expected number of times that the (a, b) configuration of the father's chromosome contributed to a particular diploid count (this is the same value for the mother, n_2, because they are assumed to be from the same haplotype distribution).

and a maximization step of:

$$D_{(a,b)} = \sum_{(i,j)} C_{(i,j)} * [n_1 + n_2]$$

$$\hat{h_{(a,b)}} = \frac{D_{(a,b)}}{\sum_{a,b} D_{(a,b)}}$$

where $D(a,b)$ is the sum of the probabilities of a particular haplotype configuration over all diploid count configurations.

We initially set all $h(a,b)$ to be 0.25 and then iterated through the algorithm until convergence (using a squared distance summed over all SNPs and a threshold of 0.001). We then used this estimate of $\tilde{p}$ to get an estimate of q.

To estimate α, we used the equation:

$$T = (1-2\alpha' + 2\alpha'^2)q + 2\alpha'(1-\alpha')p$$

Here T is the distribution underlying the observed haplotypes of the test individual and α' is the contamination ($'$ is used to indicate that this is an estimate of the real α). q is the haplotype distribution for an uncontaminated sample. A fraction $(1 - \alpha')^2 + \alpha'^2$ of the distribution should look like this, where $(1 - \alpha')^2$ is the probability that two uncontaminated sequences form the SNP pair and α'^2 is the probability that two contaminated sequences form the SNP pair, assuming the contaminating sequences are from a single individual, which would “re-form” a

596 SNP pair with LD (note: this also makes the simplifying assumption that the contaminant and
597 the test individual have the same background haplotype and SNP distribution). *p* is the
598 distribution of unrelated "haplotypes" that would form by chance from background allele
599 frequencies in the population. Contamination would form these unrelated haplotypes by
600 breaking up LD, so $2\alpha'(1 - \alpha')$ percent of the distribution should look like this (i.e. the probability
601 that the SNP pair is formed from a contaminated sequence and an uncontaminated sequence).
602
603 This equation can be used to solve for α' by maximizing the LOD (log of the odds) scores under
604 the null hypothesis that $\alpha' = 0$ and the alternative hypotheses of different α'. A LOD score is
605 assigned to each estimate of the contamination rate (α) between -0.1 to 0.5 (negative scores
606 are included to allow correction for inbreeding). The α' with the highest LOD score is the best
607 estimate of α, and is returned. When we have multiple sequences on the same SNP we assume
608 independence of the sequences, which provides additional power. The assumption of
609 independence does not bias the error estimation for the same reason as explained above for
610 independence of SNP pairs.
611
612 In practice, the α' that we obtain is not equal to the true α, because the reference panel does not
613 perfectly capture the SNP and haplotype frequencies of the test sample. We found that this
614 difference causes a linear shift in contamination estimate where the mismatch between the
615 sample individual and the reference panel leads to a positive shift while inbreeding leads to a
616 negative shift. These biases can be addressed in either of two ways.
617
618 First, for the "damage correction" approach, we performed an α' estimate only on sites from
619 sequences with evidence of damage characteristic of ancient samples. These sites do not have
620 present-day contamination and thus the α' calculated would be the linear shift, which can be

621 subtracted out from the estimate based on all sites. We separately analyzed the following pairs
622 of SNPs: UU (both SNPs at undamaged sequences), DU (one site damaged and the other
623 undamaged), and DD (both SNPs at damaged sequences). For the UU pairs, the value we
624 calculate would be α + k, where k is the linear shift. For DU pairs the value calculated would be
625 $\alpha/2$ + k, and for DD pairs the value calculated would be k. We added the likelihoods for these
626 pairs and maximized the likelihood to solve for α and k. After solving for α, we multiply by (1-
627 damage rate) to obtain the contamination level across all sequences, because α is the
628 contamination rate at undamaged sequences.
629
630 Second, for the "external correction" approach, we took samples of the sample population that
631 were high coverage and samples we believed had very low contamination (based on X
632 chromosome estimates with *ANGSD*) and measured α'. We assumed a true contamination of 0
633 for these samples and thus subtracted this α' from all other contamination estimates.
634
635
636 **Data simulation:**
637
638 To test the accuracy of the algorithm, we applied it to a variety of scenarios with both present-
639 day DNA as well as real aDNA samples that had simulated present-day DNA contamination. In
640 all our simulations with 1000 Genomes individuals, we removed the individual being used from
641 our haplotype panel before performing the analyses.
642
643 *Simulated Contamination of Present-day Individuals:*
644 We first simulated contamination of present-day individuals with other present-day individuals as
645 contaminants (this allowed us to be sure that there was no baseline contamination). In order to
646 best approximate the distribution of both the damaged and undamaged sequences that is

647 characteristic of aDNA data, we used sequence-depth information from an ancient individual as
648 a reference. At each SNP, the total number of simulated “damaged” and “undamaged”
649 sequences was determined based on the number of damaged and undamaged sequences at
650 the SNP in the reference ancient individual. The identity of each allele for the present-day
651 “base” sample was randomly chosen based on the genotype of the “base” present-day 1000
652 Genomes individual at each SNP, as described above for the contamination. The addition of
653 contaminant sequences to the dataset was performed using the method described above. In
654 order to reduce bias caused by the damage correction procedure, the damage restricted dataset
655 was generated only once for each simulation type (which included multiple simulations across
656 varying contamination rates) and combined with the undamaged dataset to produce the overall
657 dataset. This method was used to generate a simulated individual using present-day CEU
658 (NA06985) or ASW (NA19625) from the 1000 Genomes dataset as the “base” sample from the
659 sequence distributions of a 1.02x coverage ancient Iberian individual (I3756) (the “reference”)
660 (14). The CEU (NA06984) individual was used as “contaminant” in each case.
661
662 In addition, we generated simulated data with contamination from multiple sources by adjusting
663 the present-day contamination simulation method to randomly sample from two or more
664 present-day source contaminant genomes with equal probability. In each case, a 1000
665 Genomes Project CEU individual (NA06985) was used as a “base” genome with the sequence
666 distribution of I3756 (the “reference”). In the case of 2 sources of contamination (Supplementary
667 Figure 5), two CEU individuals from the 1000 Genomes Project dataset (NA06984 and
668 NA06986) were used as contamination sources, and in the case of three contamination
669 sources, an additional CEU individual was used (NA06989). Data was generated for all
670 combinations of undamaged contamination rates, α, from 0-15%.
671
672

673 *Simulated contamination of ancient individuals:*

674 We performed two sets of simulations contaminating different ancient individuals. In both cases
675 we selected ancient male individuals with minimal contamination (as assessed by X
676 chromosome contamination levels from *ANGSD* (12)) to act as the "base" uncontaminated
677 genome. In the first simulation set, we tested *ContamLD*'s performance with different ancient
678 individuals and different present-day contaminant individuals from the 1000 Genomes dataset
679 (20) to assess the impact of contaminant ancestry and coverage of the ancient individual. In this
680 case we were only using *ContamLD* and thus we performed the simulated contamination on the
681 genotype level. In the second simulation set, we compared *ContamLD* to *ANGSD* and used a
682 ~1200BP ancient West Eurasian individual (I10895) to contaminate the BAM files directly.
683

684 In the first simulation set, we used the fact that sequences with C-to-T damage are highly
685 unlikely to be the product of contamination except in the context of cross-contamination by
686 another ancient DNA sample. Thus, we exclusively added contamination to the "undamaged"
687 fraction of sequences. At each SNP site, we classified sequences present in the damage
688 restricted dataset as "damaged" and added to the simulated SNP data. We classified all other
689 sequences as "undamaged" and also added them to the simulated SNP data, but for each
690 "undamaged sequence" we added a contaminant sequence to the simulated SNP data with
691 probability $\alpha/(1-\alpha)$, where α is equal to the contamination rate (since the added sequences
692 contribute to the total number of sequences, we needed to add a higher proportion than the
693 contamination rate to obtain our desired contamination rate). The identity of the added
694 contaminant allele was randomly chosen based on the genotype of the chosen "contaminant"
695 present-day genome at the site (i.e. if the contaminant individual was homozygous at the site,
696 the allele it possesses would be added to the simulated individual, while if it were heterozygous
697 at the site, either the reference or alternative allele would be selected randomly and added to
698 the simulated individual). This method maintains the underlying distribution of "uncontaminated"

699 reference and alternative alleles at each SNP site, while adding additional “contaminant” alleles
700 to each site, producing an overall contamination rate of α in the undamaged sequences. For
701 each simulation, we generated two output files: (1) a file reporting the total number of
702 sequences carrying reference and alternative alleles at each SNP and (2) a damage restricted
703 file reporting the total number of damaged sequences carrying reference and alternative alleles
704 at each SNP. We used a 1.02x coverage ancient Iberian individual (I3756) (Supplementary
705 Online Table 1) with contamination from either the 1000 Genomes CEU individual NA06984, the
706 TSI individual NA20502, the CHB individual NA18525, or the YRI individual NA18486. We also
707 used 5 other ancient individuals, I1845 (an ancient Iberian sample of 0.46x coverage) (14),
708 I2743 (an ancient Hungarian of 0.27x coverage) (25), I5891 (a Neolithic Ukranian individual of
709 0.016x coverage) (30), DA362.SG (a Russian early Neolithic Shamanka East Asian individual of
710 1.10x coverage) (16), and I9028.SG (a South African individual of 1.21x coverage) (17). In each
711 case, we simulated individuals with 0-15% contamination.
712
713 For the second simulation set, we analyzed 65 ancient individuals of average coverage over
714 0.5X and baseline *ANGSD* estimates under 2% (Supplementary Online Table 2). In these
715 cases, we added artificial contamination with sequences from a ~1200BP ancient West
716 Eurasian individual (I10895) into the BAM files at the amounts: (0.000, 0.005, 0.010, 0.020,
717 0.025, 0.030, 0.040, 0.050, 0.060, 0.070, 0.080, 0.090, 0.100, 0.150). We removed two base
718 pairs from the end of each sequence of partial UDG treated samples and ten nucleotides for
719 non-UDG treated samples and pulled down the genotypes by randomly selecting a single
720 sequence at each site covered by at least one sequence in each individual to represent the
721 individual’s genotype at that position (“pseudo-haploid” genotyping). To ensure that the damage
722 sequences were only from the non-contaminant individual (so that we could use the damage
723 restricted correction mode, option 1, of *ContamLD* without bias), we created the “damaged”
724 sequence set as a randomly chosen 5% of the sequences from the non-contaminant individual.

725 We then analyzed the data with *ContamLD* (damage restricted correction version, option 1) and
726 *ANGSD* using default settings (Method 1).
727
728 As a last simulation, we tested the case of an ancient individual contaminating another ancient
729 individual where some of the damaged sequences would also come from the contaminating
730 individual. In this simulation, we analyzed a 1.02x coverage ancient Iberian individual (I3756)
731 and contaminated the BAM with sequences from a ~1200BP ancient West Eurasian individual
732 (I10895) at the amounts: (0.000, 0.005, 0.010, 0.020, 0.025, 0.030, 0.040, 0.050, 0.060, 0.070,
733 0.080, 0.090, 0.100, 0.150, 0.200, 0.300). We then down-sampled the BAM, taking a random
734 5% of the sequences of these contaminated BAM files to act as the "damaged" sequences,
735 because this would naturally correct for any baseline contamination in the I3756 individual yet
736 would simulate additional contamination of I3756 by an ancient individual with the same
737 damage rate as I3756 (i.e. if there is 5% contamination, then also 5% of the damaged
738 sequences would be from the contaminant individual in this simulation). We then performed the
739 standard pull-down on both the full contaminated BAMs and the 5% down-sampled BAMs
740 (simulated to be "damaged" sequences), removing two base pairs from the end of each
741 sequence and doing a "pseudo-haploid" genotype pulldown. We ran *ContamLD* on the resulting
742 data with damage restricted correction, option 1.
743
744 *Direct Analyses of Contamination Levels in Ancient Individuals:*
745 As our last set of analyses, we directly measured contamination levels in ancient individuals
746 without simulated contamination. We used *ContamLD* to analyze shotgun sequenced
747 individuals pulled down onto the 1240K SNP set and the shotgun panel created using all
748 variants above 10% frequency in the 1000 Genomes dataset. The ancient shotgun sequenced
749 individuals were of 0.1-0.5x coverage from Allentoft *et al*., 2015 (26), Damgaard *et al.*, Nature
750 2018 (31), and Damgaard *et al*., Science 2018 (16). In addition, we analyzed 439 individuals

751 from a variety of ancestries with *ContamLD* (damage corrected version), *ANGSD* (12, 32) using
752 default settings (we report the results from Method 1), and *contamMix* (33) with the settings:
753 down-sampling to 50X for samples above that coverage, --trimBases X (2 bases for UDG-half
754 samples and 10 bases for UDG-minus samples), 8 threads, 4 chains, and 2 copies, taking the
755 first one that finishes. Supplementary Online Table 1 includes all information from these
756 individuals.

757

758 # Declarations

759

760 **Ethics Approval and Consent to Participate**

761 Not applicable (all samples were from previously published studies).

762

763 **Consent for publication**

764 Not applicable.

765

766 **Availability of Data/Materials and Requirements:**

767 All data analyzed in this article are available in (2, 16, 17, 22-28, 31). The software is available
768 at: https://github.com/nathan-nakatsuka/ContamLD. It requires Python 3 and R (any version
769 should suffice). Scripts for data simulations are available upon request.

770

771 **Competing interests:**

772 The authors declare that they have no competing interests.

773

774

775 **Funding:**

776 Funding was provided by an NIGMS (GM007753) fellowship to NN and a MHAAM fellowship to
777 EH. DR is an Investigator of the Howard Hughes Medical Institute and this work was supported
778 by grants HG006399 and GM100233 from the National Institutes of Health and by grant 61220
779 from the John Templeton Foundation.

780

781 **Authors' Contributions:**

782 N.N., E.H., N.P., and D.R. conceived the study. N.N., E.H., and S.M. performed analysis. N.N.,
783 E.H., and D.R., wrote the manuscript with the help of all co-authors.

784

785 **Acknowledgements:**

786 We thank Iosif Lazaridis and Mark Lipson for helpful discussions.

787 # References

788 1. Dabney J*, et al.* (2013) Complete mitochondrial genome sequence of a Middle
789 Pleistocene cave bear reconstructed from ultrashort DNA fragments. *Proc Natl Acad Sci*
790 *U S A* 110(39):15758-15763.
791 2. Haak W*, et al.* (2015) Massive migration from the steppe was a source for Indo-
792 European languages in Europe. *Nature* 522(7555):207-211.
793 3. Rohland N, Harney E, Mallick S, Nordenfelt S, & Reich D (2015) Partial uracil-DNA-
794 glycosylase treatment for screening of ancient DNA. *Philos Trans R Soc Lond B Biol Sci*
795 370(1660):20130624.
796 4. Skoglund P*, et al.* (2014) Separating endogenous ancient DNA from modern day
797 contamination in a Siberian Neandertal. *Proc Natl Acad Sci U S A* 111(6):2229-2234.
798 5. Sawyer S*, et al.* (2015) Nuclear and mitochondrial DNA sequences from two Denisovan
799 individuals. *Proc Natl Acad Sci U S A* 112(51):15696-15700.
800 6. Fu Q*, et al.* (2013) DNA analysis of an early modern human from Tianyuan Cave, China.
801 *Proc Natl Acad Sci U S A* 110(6):2223-2227.
802 7. Green RE*, et al.* (2008) A complete Neandertal mitochondrial genome sequence
803 determined by high-throughput sequencing. *Cell* 134(3):416-426.
804 8. Green RE*, et al.* (2010) A draft sequence of the Neandertal genome. *Science*
805 328(5979):710-722.
806 9. Cibulskis K*, et al.* (2011) ContEst: estimating cross-contamination of human samples in
807 next-generation sequencing data. *Bioinformatics* 27(18):2601-2602.
808 10. Jun G*, et al.* (2012) Detecting and estimating contamination of human DNA samples in
809 sequencing and array-based genotype data. *Am J Hum Genet* 91(5):839-848.
810 11. Racimo F, Renaud G, & Slatkin M (2016) Joint estimation of contamination, error and
811 demography for nuclear DNA from ancient humans. *PLoS genetics* 12(4).

12. Korneliussen TS, Albrechtsen A, & Nielsen R (2014) ANGSD: Analysis of Next Generation Sequencing Data. *BMC Bioinformatics* 15:356.

13. Mathieson I*, et al.* (2015) Genome-wide patterns of selection in 230 ancient Eurasians. *Nature* 528(7583):499-503.

14. Olalde I*, et al.* (2019) The genomic history of the Iberian Peninsula over the past 8000 years. *Science* 363(6432):1230-1234.

15. Seguin-Orlando A*, et al.* (2014) Genomic structure in Europeans dating back at least 36,200 years. *Science* 346(6213):1113-1118.

16. de Barros Damgaard P*, et al.* (2018) The first horse herders and the impact of early Bronze Age steppe expansions into Asia. *Science* 360(6396):eaar7711.

17. Skoglund P*, et al.* (2017) Reconstructing Prehistoric African Population Structure. *Cell* 171(1):59-71 e21.

18. Patterson N*, et al.* (2004) Methods for high-density admixture mapping of disease genes. *The American Journal of Human Genetics* 74(5):979-1000.

19. Alexander DH, Novembre J, & Lange K (2009) Fast model-based estimation of ancestry in unrelated individuals. *Genome Res* 19(9):1655-1664.

20. Genomes Project C*, et al.* (2015) A global reference for human genetic variation. *Nature* 526(7571):68-74.

21. Renaud G, Slon V, Duggan AT, & Kelso J (2015) Schmutzi: estimation of contamination and endogenous mitochondrial consensus calling for ancient DNA. *Genome Biol* 16:224.

22. Lazaridis I*, et al.* (2014) Ancient human genomes suggest three ancestral populations for present-day Europeans. *Nature* 513(7518):409-413.

23. Lazaridis I*, et al.* (2016) Genomic insights into the origin of farming in the ancient Near East. *Nature* 536(7617):419-424.

24. Lazaridis I*, et al.* (2017) Genetic origins of the Minoans and Mycenaeans. *Nature* 548(7666):214-218.

838 25. Lipson M*, et al.* (2017) Parallel palaeogenomic transects reveal complex genetic history
839 of early European farmers. *Nature* 551(7680):368-372.
840 26. Allentoft ME*, et al.* (2015) Population genomics of Bronze Age Eurasia. *Nature*
841 522(7555):167-172.
842 27. Keller A*, et al.* (2012) New insights into the Tyrolean Iceman's origin and phenotype as
843 inferred by whole-genome sequencing. *Nat Commun* 3:698.
844 28. Olalde I*, et al.* (2018) The Beaker phenomenon and the genomic transformation of
845 northwest Europe. *Nature* 555(7695):190.
846 29. Purcell S*, et al.* (2007) PLINK: a tool set for whole-genome association and population-
847 based linkage analyses. *Am J Hum Genet* 81(3):559-575.
848 30. Mathieson I*, et al.* (2018) The genomic history of southeastern Europe. *Nature*
849 555(7695):197.
850 31. de Barros Damgaard P*, et al.* (2018) 137 ancient human genomes from across the
851 Eurasian steppes. *Nature* 557(7705):369.
852 32. Durvasula A*, et al.* (2016) angsd-wrapper: utilities for analysing next-generation
853 sequencing data. *Mol Ecol Resour* 16(6):1449-1454.
854 33. Fu Q*, et al.* (2014) Genome sequence of a 45,000-year-old modern human from western
855 Siberia. *Nature* 514(7523):445-449.
856

Supplementary Figures

A)

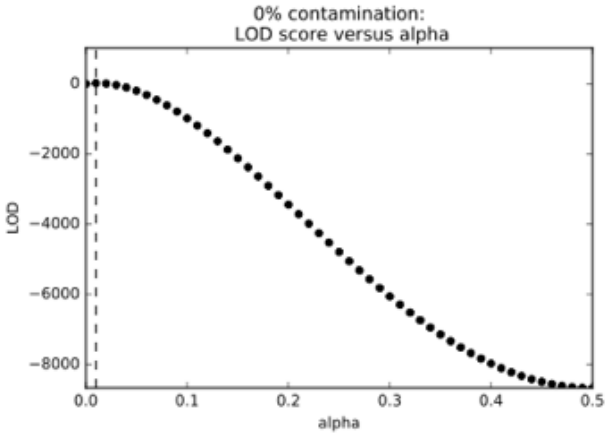

B)

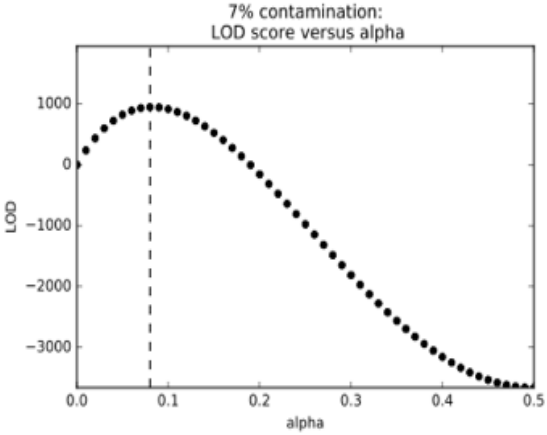

C)

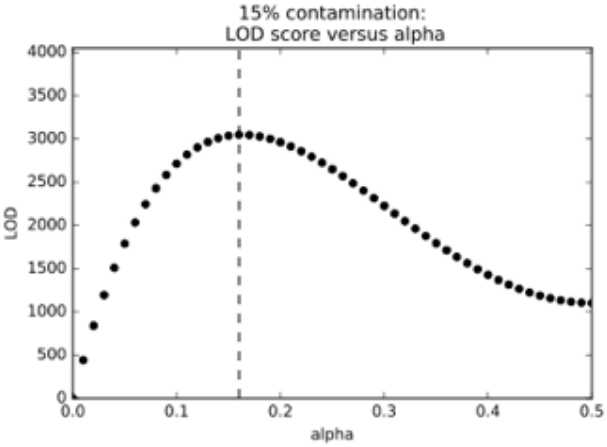

Supplementary Figure 1. Distribution of LOD scores in simulated data. The distribution of LOD scores is depicted for samples with **A)** 0%, **B)** 7%, and **C)** 15% simulated contamination. These data were generated as part of tests using 1000 Genomes CEU individuals as the sample and contaminant DNA and for the haplotype panel.

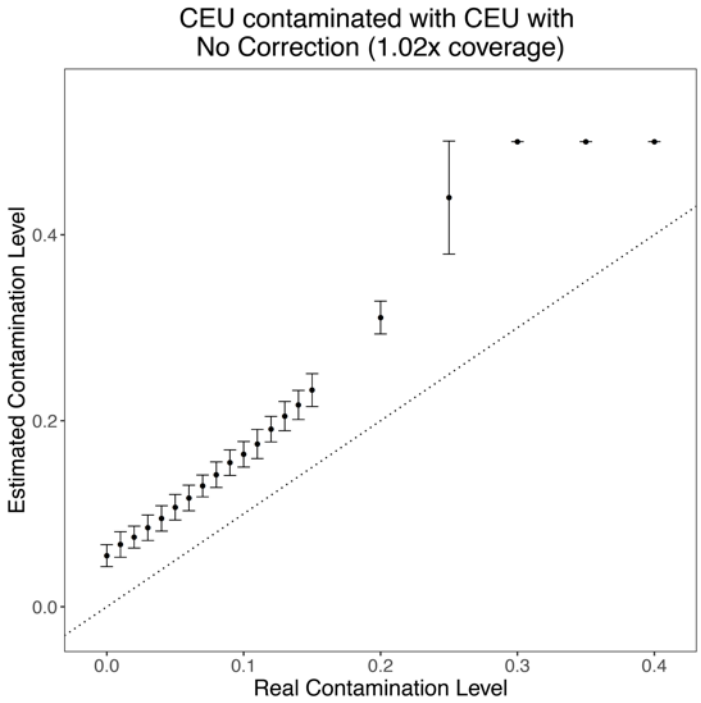

868

869 **Supplementary Figure 2. Contamination estimates when the individual, contaminant, and**

870 **haplotype panel are all from the same population (CEU) with no correction.** The black dotted line is

871 y=x, which would correspond to a perfect estimation of the contamination. Error bars are 1.96*standard

872 error (95% confidence interval).

873

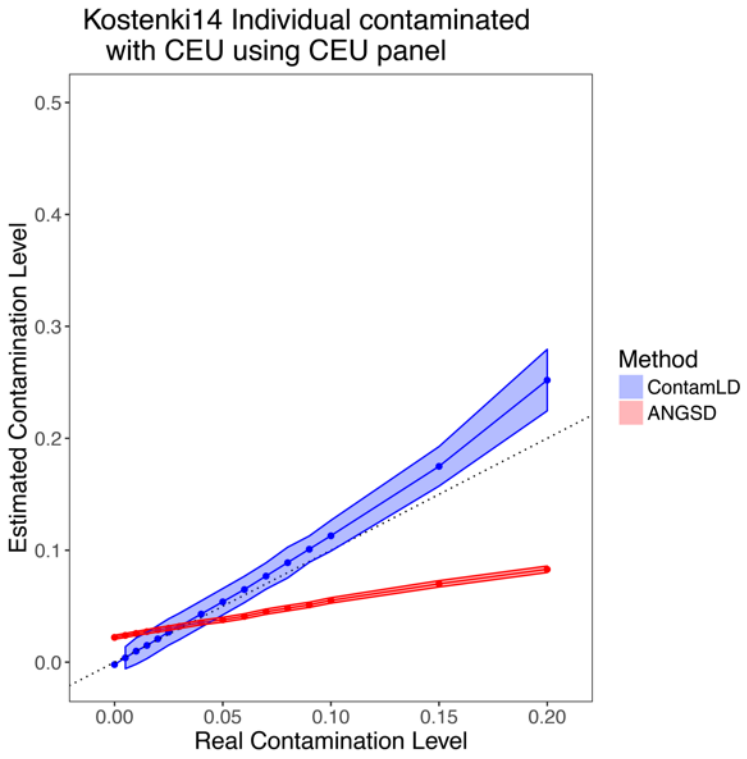

Supplementary Figure 3. Contamination estimates for Upper Paleolithic European individual after damage restricted correction (option 1). Kostenki14 (2.81x coverage) was contaminated with CEU and analyzed using a CEU panel with *ContamLD* using damage correction and *ANGSD* (12) (Method 1). The black dotted line is y=x, which would correspond to a perfect estimation of the contamination. Error shading is 1.96*standard error (95% confidence interval).

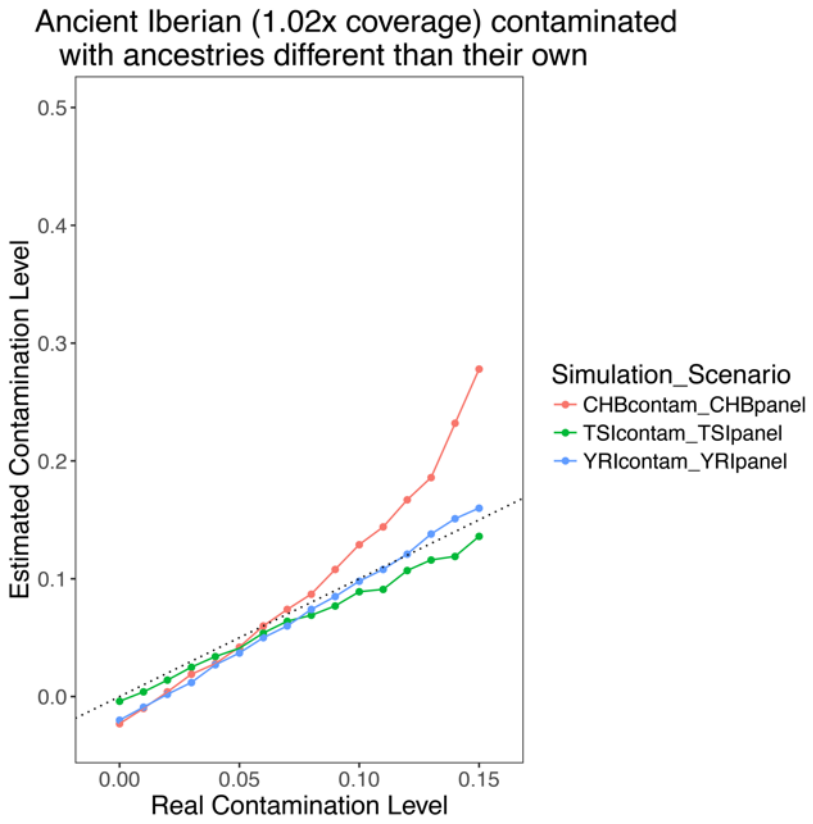

Supplementary Figure 4. Contamination estimates with an ancient European as the sample and ancestry matched contaminants and haplotype panels with damage restricted correction (option 1). An ancient Iberian of 1.02x coverage (I3756) is analyzed in 3 different situations: 1) contaminated with TSI and analyzed with a TSI panel, 2) contaminated with CHB and analyzed with a CHB panel, and 3) contaminated with YRI and analyzed with a YRI panel. The black dotted line is y=x, which would correspond to a perfect estimation of the contamination.

897 **A)** **B)**

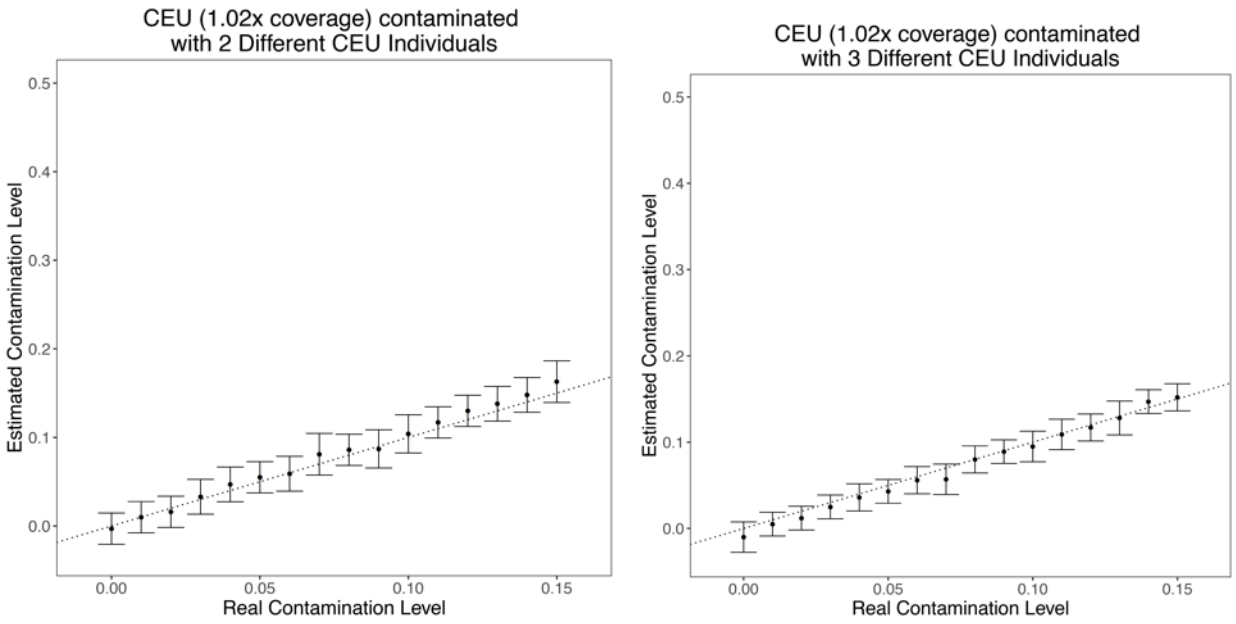

898

899 **Supplementary Figure 5. Contamination estimates with CEU as the sample and multiple CEU**

900 **individuals as contaminants analyzed with CEU haplotype panels with damage restricted**

901 **correction (option 1).** A CEU individual of 1.02x coverage (from the sequence distribution of the ancient

902 Iberian above) is contaminated with **A)** two CEU individuals or **B)** three CEU individuals. The black dotted

903 line is y=x, which would correspond to a perfect estimation of the contamination. Error bars are

904 1.96*standard error (95% confidence interval).

905

906

907

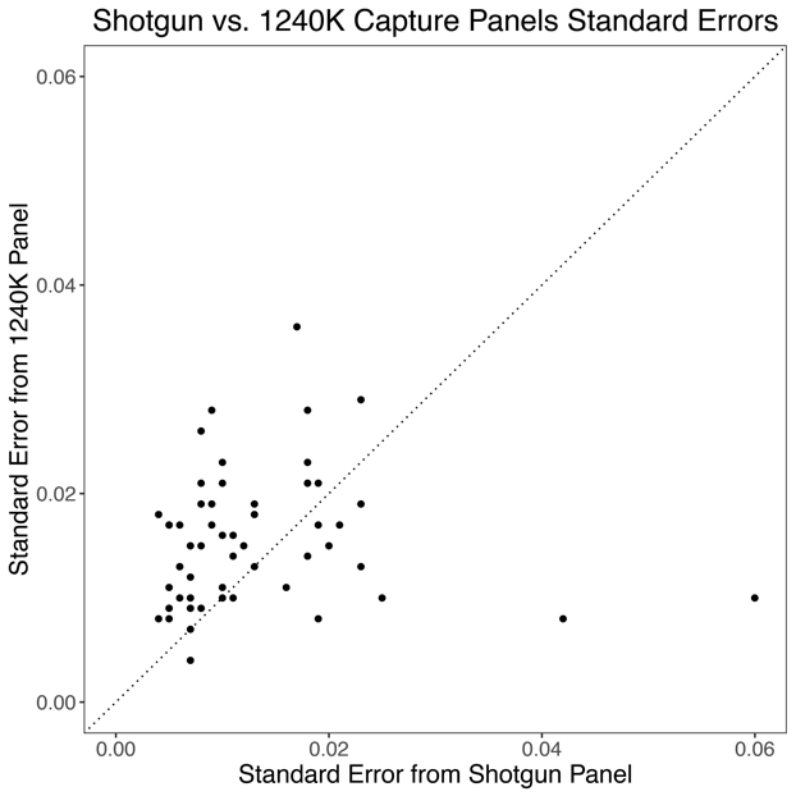

Supplementary Figure 6. Contamination estimate standard errors of shotgun sequenced ancient individuals comparing the 1240K panel to the shotgun panel. Ancient shotgun sequenced individuals of 0.1-0.5x coverage from Allentoft *et al*., 2015 (26), Damgaard *et al.*, Nature 2018 (31), and Damgaard *et al*., Science 2018 (16) were analyzed with *ContamLD* damage restricted correction (option 1) using the 1240K SNP set and a shotgun panel created using all variants above 10% frequency in the 1000 Genomes dataset. This test shows that analyses with the shotgun panel generally have smaller error bars relative to those done with the 1240K panel, though it is unclear why there are two outliers with high standard errors on the shotgun panel and low standard errors on the 1240K panel. All estimates are in Supplementary Online Table 1.

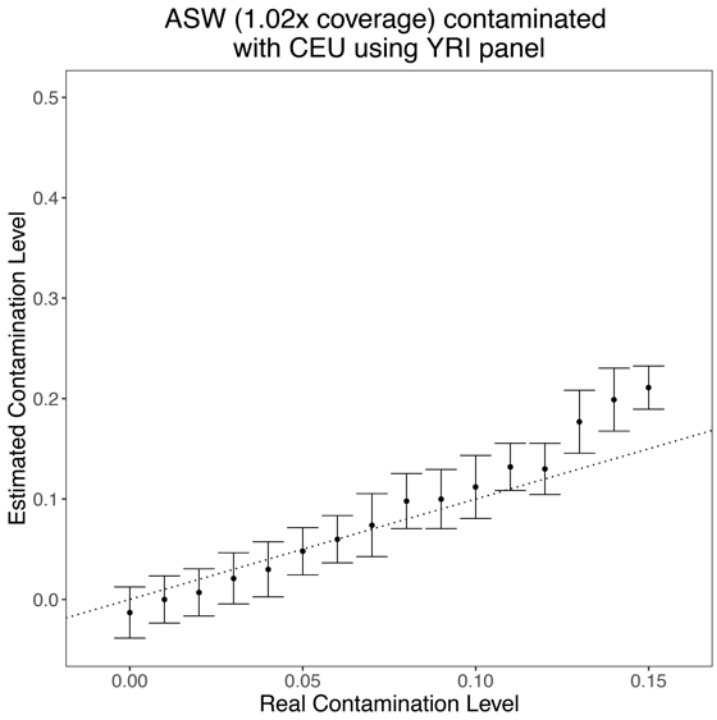

Supplementary Figure 7. *ContamLD* estimates with an ASW (African-American) individual and YRI panel using damage restricted correction (option 1). The black dotted line is y=x, which would correspond to a perfect estimation of the contamination. Error bars are 1.96*standard error (95% confidence interval).

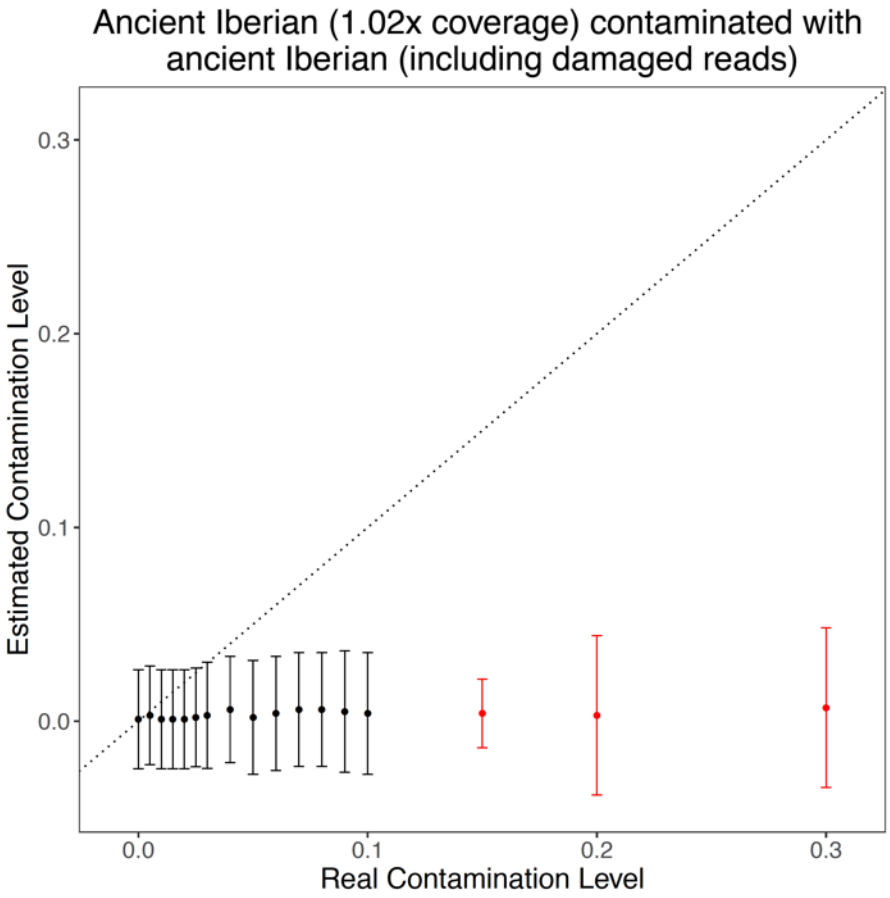

928

929 **Supplementary Figure 8. *ContamLD* estimates with an ancient Iberian (I3756) individual**
930 **contaminated with an ancient Iberian (I10895) including its damaged sequences analyzed with IBS**
931 **panel using damage restricted correction (option 1).** The damaged sequences were simulated as a
932 5% down-sampling of each respective contaminated BAM file. IBS are 1000 Genomes Project present-
933 day Iberians from Spain. The black dotted line is y=x, which would correspond to a perfect estimation of
934 the contamination. Error bars are 1.96*standard error (95% confidence interval). Points in red are those
935 flagged with "Very_High_Contamination" by the software. See Supplementary Online Table 4 for all
936 values.